J Mol Model (2009) 15:607–613
DOI 10.1007/s00894-008-0438-1

ORIGINAL PAPER

Structural and energetic heterogeneities of canonical and oxidized central guanine triad of B-DNA telomeric fragments

Piotr Cysewski · Przemysław Czeleń

Received: 25 August 2008 / Accepted: 5 December 2008 / Published online: 9 January 2009

Abstract The intermolecular interaction energies in central guanine triad of telomeric B-DNA were estimated based on ab initio quantum chemistry calculations on the MP2/aDZ level of theory. The source of structural information was molecular dynamics simulation of both canonical (AGGGTT) and oxidized (AG8oxoGGTT) telomere units. Our calculations demonstrate that significant stiffness of central triad occurs if 8oxoG is present. The origin of such feature is mainly due to the increase of stacking interactions of 8oxoG with neighbouring guanine molecules and stronger hydrogen bonding formation of 8oxoG with cytosine if compared with canonical guanine. Another interesting observation is the context independence of stacking interactions of 8oxoG. Unlike to 5′-G_2/G_3-3′ and 5′-G_3/G_4-3′ sequences which are energetically different, 5′-G_2/8oxoG_3-3′ and 5′-8oxoG_3/G_4-3′ sequences are almost iso-energetic.

Keywords GGG triad · Oxidative damage · 8-oxo-guanine · Stacking · Telomers

Introduction

Intermolecular interactions determine structure and properties of many crucial biomolecules [1, 2]. The cellular enzymatic machinery relies on subtle energetic effects during recognition, repairing, replication, synthesis and many other life-sustaining processes. One of such example are telomeric fragments present in every human somatic cell [3, 4]. They play an intricate role of "mitotic clock" due to their regular shortening with each cell division by about 20–200 base pairs [5–7]. This vital structure is protected by DNA binding proteins, TRF1 [8] and TRF2 [9]. There is observed intricate sensibility of such DNA-protein complexes formation on the presence of 8-oxo-guanine in telomeric DNA [10, 11]. Even single lesion reduces by a factor two the ability of protein binding in comparison with standard non-damaged DNA [12]. The presence in telomeric repeats of multiple 8-oxo-guanine lesions, has more dramatic consequences and makes the binding process nearly impossible. Although in one of our previous papers [13] some comments on the structure and energy of oxidized telomeric fragments were provided there are still open questions that deserve further investigations. First of all the structure of B-DNA is controlled by two distinct intermolecular interactions, namely hydrogen bonding and stacking interactions [14–18]. Despite significant progress in contemporary force field the empirical formula posses inherent pitfalls [19], which prevent direct use in precise characteristic of the intermolecular interactions. Thus, only quantum chemistry methodology provide rationale tools for accurate characteristics of the base-base interactions [20–22]. The hydrogen bonding is governed mainly by electrostatic contribution and may be properly described by modest levels of theory [20–22]. On the contrary for proper characteristics of stacking interactions only advanced ab initio levels including electron correlation are of choice [20–24]. This is related to significant contribution of London dispersions to the stacking interactions [25]. Furthermore, both hydrogen bonding and stacking of nucleobases are very sensitive to mutual orientation of monomers [26]. Since the stability and flexibility of B-DNA double helix relies on delicate interplay of different

P. Cysewski (✉) · P. Czeleń
Physical Chemistry Department, Collegium Medicum,
Nicolaus Copernicus University,
Kurpińskiego 5,
85-950 Bydgoszcz, Poland
e-mail: piotr.cysewski@cm.umk.pl

energetic components [2, 27] the selection of representative conformation(s) is not a trivial task [28]. For demonstration purposes in Fig. 1 there were presented the fluctuations of values of selected base step parameters observed during molecular dynamics simulations of 5′-ACTTAGGGT TAGGG-3′ sequence. More technical details are provided below in the methodology part. It is essential to notice that although there are correlations between values of step parameters the broad range of conformations are typically adopted by nucleobases in B-DNA. Obviously there is not just one set of base step parameters and their mean values are simply meaningless. Thus, in order to characterize the intrinsic intermolecular interactions in the telomeric B-DNA fragments the broad spectrum of conformations must be taken into account. Thus, the aim of this study is the statistical analysis of intermolecular interactions occurring in the standard and oxidized telomeric fragments. Besides, the structural imposed changes cased by guanine oxidation are also discussed.

Methods

The conformations of two nucleobases pairs are controlled in B-DNA double strand by the set of 18 parameters [29, 30]. The mutual orientation of hydrogen-bonded pairs is declared by *shear*, *stretch*, *stagger*, *buckle*, *propeller* and *opening*, while the values of *shift*, *slide*, *rise*, *tilt*, *roll* and *twist* define the base-base orientations in stacked conformations. The contemporary instrumental methods as NMR or Xray diffraction may directly provide these data [31]. Although there are numerous NMR experiments [32, 33] on non-modified telomeric fragments such data are unavailable for oxidized chains. Fortunately, the molecular dynamics simulations may also be used as a source of values of the base pair and base step parameters. The AMBER [34] force-field is widely and successfully used for studying of the time evolutions of variety model systems [35–38]. In this paper the trajectories generated during 2000 ps runs were used for quenching of snapshots. Thus, B-DNA double helix sequences (str.1: 5′-ACTTA$_1$G$_2$G$_3$G$_4$T$_5$T6AGGG-3′, str.2: 5′-ACTTA$_1$G$_2$8oxoG$_3$G$_4$T$_5$T$_6$AGGG-3′) were built based on standard parameters [39]. Each structure was immersed in a 54 Å×52 Å×75 Å box filled with 4893 water molecules and 26 sodium cations. The periodic boundary conditions were applied for 2500 ps simulations at room temperature. Initial 500 ps interval was sufficient for equilibration in either case. This was confirmed by stable fluctuations of RSMD and energies values. The structural parameters were collected every 1 ps for final 2000 ps. The B-DNA base pair and base step parameters were estimated using X3DNA program [39] for each snapshot. These data were used for characteristics of structural diversities of standard and oxidized central telomeric triad (CTT) comprising 5′-G$_2$G$_3$G$_4$-3′ or 5′-G$_2$8oxoG$_3$G$_4$-3′ sequences. The intermolecular interaction energies (IIE) were estimated for every 20 ps snapshots. The X3DNA program was used for generation of stacked and hydrogen bonded pairs. The

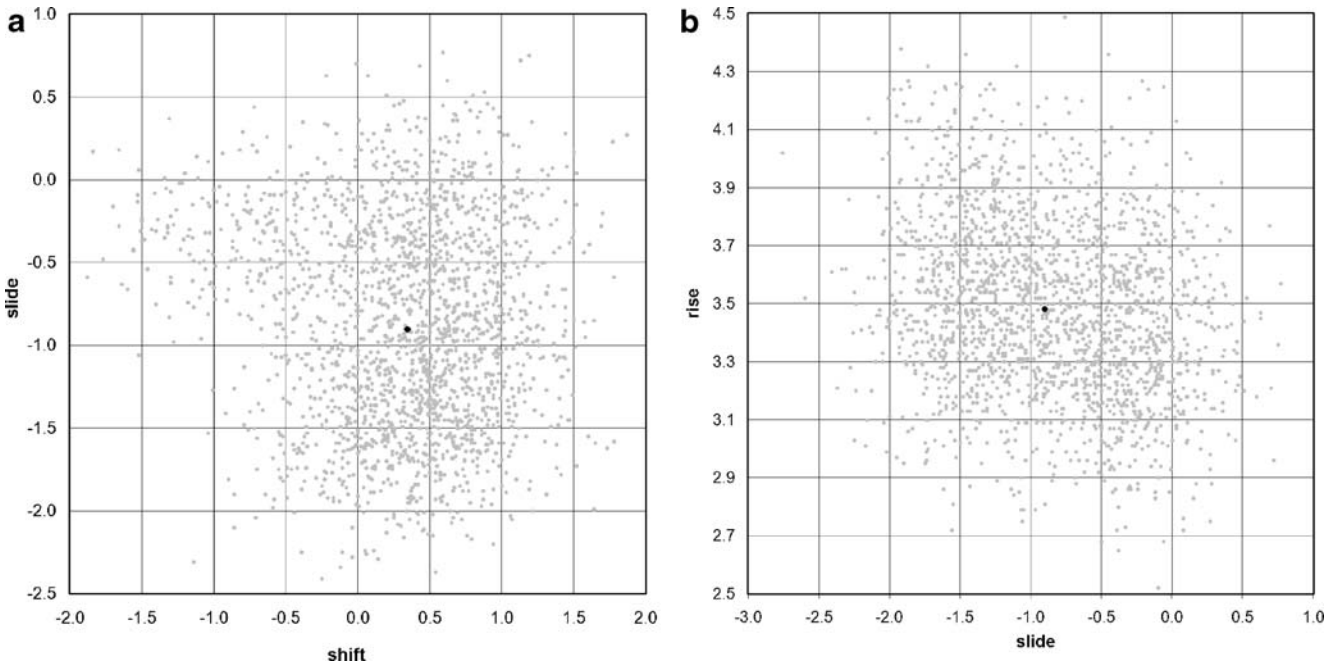

Fig. 1 The fluctuations of values of selected displacement parameters defining mutual conformations of G2/G3 guanine molecules in 5′-ACTTA$_1$G$_2$G$_3$G$_4$T$_5$T$_6$AGGG-3′ sequence. The MD simulation details are provided in the methodology part. Grey dots represent values corresponding to snapshots taken every 1 ps from MD runs. The black point stands for averaged value over 2000 ps

structures of nucleobases originally defined in the 3XDNA local library (without hydrogen atoms) were modified and replaced with ones optimized at MP2/aug-cc-pVDZ level. The planarity (Cs symmetry) of canonical bases was imposed during gradient optimization of monomers geometry. Then all atoms were removed except the ones belonging to stacked or hydrogen bonded pairs. In such a way the sugar-phosphate backbones were simplified just by hydrogen atoms. Thus, 100 structures corresponding to either G_2/G_3, G_3/G_4, $8oxoG_2/G_3$, $8oxoG_3/G_4$ stacking or G_3-C, $8oxoG_3$-C hydrogen boding were used for IIE estimation at DF-MP2/aug-cc-pVDZ (aDZ) level of theory. The density fitting (DF) method was applied since it is about one order of magnitude faster than the exact MP2 treatment and provides almost identical values of the intermolecular interaction energies as MP2 level. The counterpoise correction for BSSE error [40, 41] was included in all single point calculations. In all molecular dynamics simulations the AMBER package [42] was used and the quantum chemistry calculations were performed with the aid of MolPro package [43].

Results and discussion

The influence of guanine oxidation on structural properties of central telomeric triad

The trajectories generated during MD simulations were used as a source of the values of base pair and base step parameters. The fluctuations of these values stand for inherent structural heterogeneities of the central telomeric triad. In order to gain deeper insight into time evolution of the CTT conformations, the statistical analysis was applied to all sets of parameters coming from 2000 ps runs. The *skewness* is often used as a measure of the asymmetry of a distribution. For a normal distribution it is equal to zero, and any symmetric data should have a *skewness* close to zero. The negative values of *skewness* indicates that the left tail of distribution is more pronounced that the right one. On the contrary positive values of *skewness* is accomplished with the presence of significant tail at higher values than median. In Fig. 2 there are presented values of *skewness* corresponding to parameters distributions estimated for both standard (str1) and oxidized (str2) central telomeric triad. As it may be inferred form Fig. 2 most of pair and step parameters are characterized by small and positive values of *skewness*. This suggests that configurational space is almost equally covered by parameters values defining structure of central telomeric triad and there is only small tail corresponding to higher values of structural parameters defining nucleobases positions in the double stranded B-DNA. However, some intriguing exceptions may be noticed. For example *shear* distribution is significantly affected by oxidation of G_3 guanine. The positive value of *skewness* is typical for non-oxidized guanine, while negative value is noticed for $8oxoG_3$. The median values of *shear* are almost the same for str1 and str2 and are equal to −0.21 Å and −0.19 Å, respectively. Since *shear* defines mutual in-plane displacement of two bases of a pair along shorter molecular axis, the right tail of the this base pair distribution suggests significant oscillations of guanine G_3 towards major groove. On the contrary the existence of the left tail of *shear* distribution is caused by occasional withdrawal of 8oxoG from the major groove towards minor groove. Besides, *opening* is also affected by oxidation of the central telomeric triad. First of all the medians are not very different and are equal to 0.11° for G_3 in str1 and −1.06° for $8oxoG_3$ in str2. The additional increase of the *skewness* of the *opening* distribution suggests more frequent rotation of 8oxoG-C pair by opening the hydrogen bonds occasionally destabilizing interactions between these two monomers. The next significant impact of the oxidation of guanine in GGG triad is the observed increase in skewness of the *roll* distributions. It has a meaning of the rotation of two successive base pairs about longer molecule axis by opening

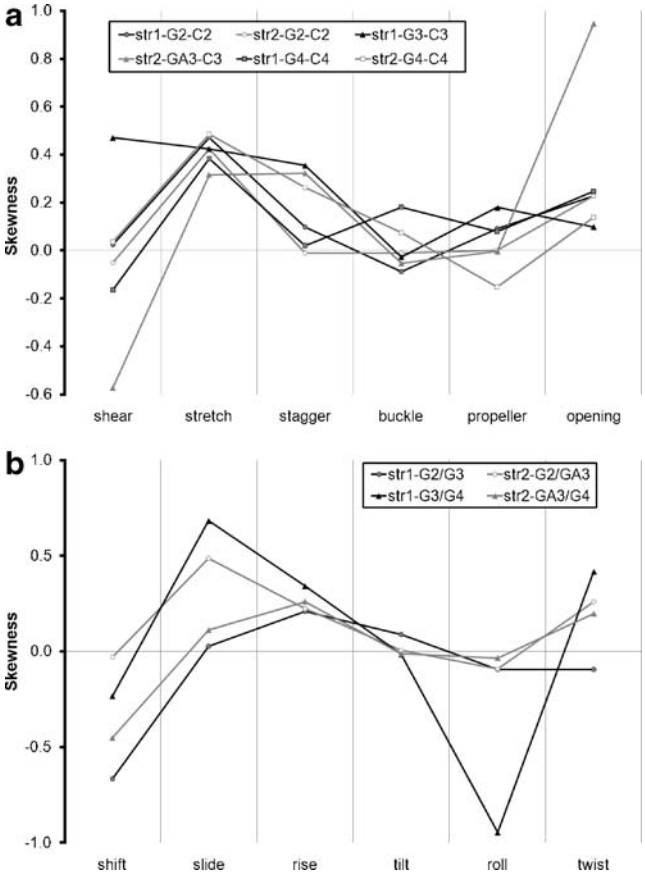

Fig. 2 The values of *skewness* of base pair and base step parameters distributions estimated for 2000 ps MD runs. The sequence of canonical telomeric fragment ($A_1\mathbf{G_2G_3G_3}T_5T_6$) is denoted as *str1*, while oxidized form ($A_1\mathbf{G_2 8oxoG_3}G_4T_5T_6$) is described as *str2*

the minor grove side. In case of G_3 in str1 the median values is equal to +5.09°, but for 8-oxoG_3 in str2 is about +6.38°. This slight increase of *roll* values is accomplished with significant increase of *skewness* of its distribution. In case of non-modified GGG triad the natural tendency of G_3 *rolling* is significantly reduced after oxidation. The *skewness* properties of the rest parameters distributions are very similar for analyzed triad in str1 and str2. Besides, the median values are also almost not affected by the oxidation of guanine molecule. The only exception is observed for *buckle*, which values are equal to 5.52° for G_3 in str1 and 2.00° for 8oxoG_3 in str2, respectively. The *buckle* denotes the rotation of two hydrogen bonded bases about shorter molecular axis. Thus, although the distributions of *buckle* are similar for both non-modified and oxidized guanines the slight increase of stiffness is observed in oxidized central telomeric triad.

The second statistical quantity characterizing distribution of structural parameters is *kurtosis*. It is a measure of whether the data are peaked or flat relative to a normal distribution. Thus, data sets with high *kurtosis* tend to have a sharp peak near the mean, decline rather rapidly, and have heavy tails. In contrast, data sets with low *kurtosis* tend to have a flat top near the mean rather than a pointed peak. A uniform distribution would be the extreme case. The *kurtosis* for a standard normal distribution equals 3.0. In case of base pair and base step parameters the high values of *kurtosis* characterize stiffness of the structure, since high percentage of conformations adopts values close to median. On the contrary low values of *kurtosis* indicates higher flexibility with respect to given parameter and greater elasticity of molecular structure. The values of *kurtosis* calculated for base pair and base step parameters distributions are presented in Fig. 3. Interestingly, most of structural parameters characterizing central telomeric triad has distribution more flat than the normal one. This suggests that these parameters fluctuate significantly during molecular dynamics simulations. The only exceptions is *opening* for 8oxoG_3-C pair, for which the values of kurtosis is close to 6.0. This consistently suggests increasing of the structural stiffness of oxidize central telomeric triad.

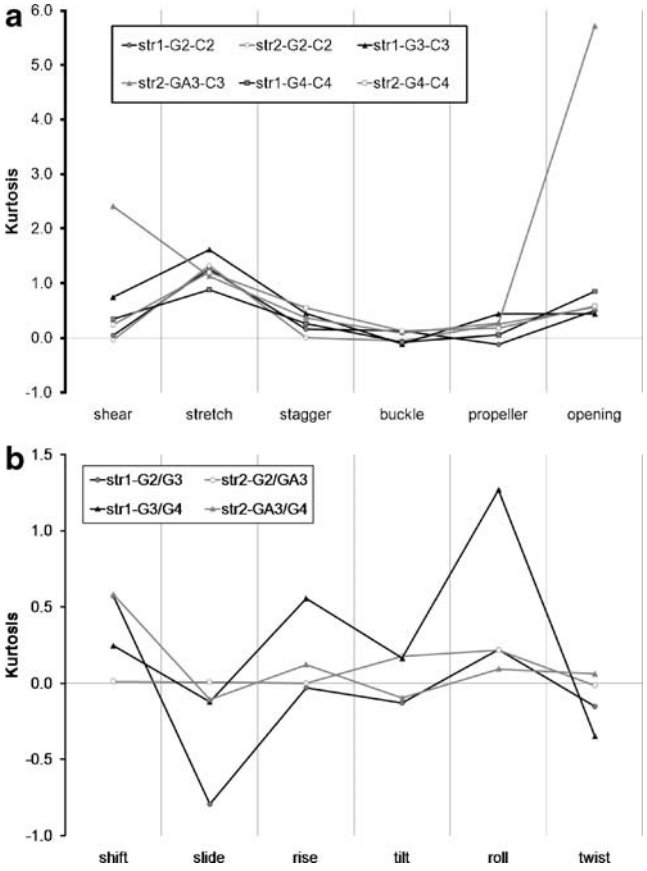

Fig. 3 The values of *kurtosis* of base pair and base step parameters distributions. Notation is the same as in Fig. 2

The stacking interactions in central telomeric triad

The structure alterations imposed by oxidation of central telomeric triad must influence the energetic characteristic of B-DNA telomeres. The distribution of intermolecular interaction energies of hydrogen bonded and stacked pairs are presented in Fig. 4. Interesting features are described by presented plots. First of all the hydrogen bonding of 8oxoG_3 with cytosine is about 2 kcal mol^{-1} stronger compared to G_3-C pair if the most probable IIE values are compared. The previously mentioned structural fluctuations of oxidized telomeric triad are also visible on the energy histograms. The presence of the significant right tail on the energy distribution is caused by *opening* and *rolling* of HB-bonded 8oxoG-pairs. Also the stacking interactions of modified guanine are stronger compared to canonical one. Interestingly, the stacking abilities of 8oxoG are context independent. Both 5′-G_3/8oxoG_4-3′ and 5′-8oxoG_3/G_4-3′ sequences are characterized by very similar IIE distributions with respect of range, shape and position of the maximums on the smoothed histograms. On the contrary, small context dependence of G/G stacking is observed due to the fact that stacking interactions in G_2/G_3 pairs seem to be slightly stronger than for G_3/G_4 pairs. It is noteworthy that stacking interactions are very important for stabilizing of CTT. Since each 8oxoG interacts with two neighbouring guanine molecules the stacking energy reached up 67% of hydrogen bonding, while for canonical guanine it makes only about 40%. Thus, the observed stiffness in oxidized CTT is mainly due to significant increase of stacking interactions. It is interesting to see what is the source of the observed differences in IIE values. The nature of intermolecular interactions may be described by detailed energy decomposition [19, 44]. Unfortunately these kind of calculations are very demanding and it is impractical to

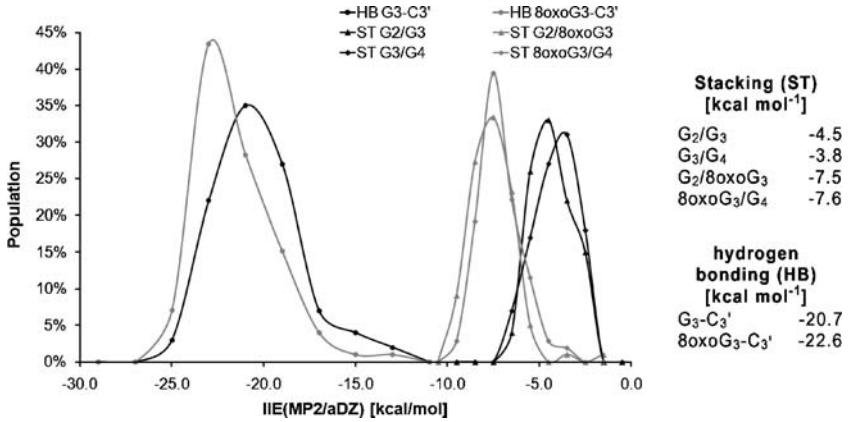

Fig. 4 The smoothed histograms presenting the distributions of intermolecular interactions occurring in canonical and oxidized central telomeric fragments. The distributions of hydrogen bonding and stacking interactions of middle purines (ie. G_3 or $8oxoG_3$) represent 100 conformations coming from 2000 ps MD runs

perform such an analysis for the set of pairs considered in this paper. However, it is noteworthy that the molecular systems stabilized mainly by electrostatic contribution may be described by one-electron approach with satisfactory accuracy. This is usually the case for hydrogen bonded systems. On the contrary if dispersion contribution becomes dominant in the intermolecular interaction energy, the electron correlation becomes crucial. Thus, the qualitative characteristics of the nature of stacking interactions may done by comparison of these two values, namely intermolecular interactions energies estimated on HF/aDZ level (denoted as IIE(HF/aDZ)), and electron correlation contribution estimated *via* MP2/aDZ approach (symbolized as IIE (corr/aDZ)). The distributions of both these terms are presented in Fig. 5. According to common expectation, the HF contribution is positive and electron correlation term is negative. However, IIE(HF/aDZ) values are lower for pairs comprising 8oxoG. This may be related to slight increase of electrostatic contribution to the stacking interactions in pairs comprising oxidized guanine. Interestingly, the electron correlation contribution is of the same magnitude for all pairs except for the G_2/G_3 one, which is characterized by higher values of this term. Furthermore, the 8oxoG is characterized by the same amount of both energy components irrespective of the context of stacking interactions. The median values of HF contribution are equal to 6.0 kcam mol^{-1} and 6.5 kcam mol^{-1} for 5′-G/8oxoG-3′ and 5′-8oxoG/G-3′ sequences, respectively. Besides, the electron correlation contribution to the total intermolecular interaction energy is also of the same magnitude and the corresponding values of medians are the following −13.9 kcam mol^{-1} and −13.7 kcal mol^{-1}. Thus, the compensation of SCF and electron correlation energies is the same and both sequences involving 8oxoG are almost iso-energetic. However, this is not the case for non-oxidized GGG triad. As it is presented in Fig. 5a the stacking interactions of G_2/G_3 pair are characterized by highest SCF component. The median values corresponding to G_2/G_3 and G_3/G_4 pairs are equal to 9.1 kcal mol^{-1} and 7.6 kcam mol^{-1}, respectively. The electron correlation contribution is slightly higher for the former pairs since the corresponding median values are equal to −13.8 kcam mol^{-1} −12.0 kcam mol^{-1}. Thus, the origin of the destabilization of G_3/G_4 pairs is due to slight decrease of SCF contribution not compensated by

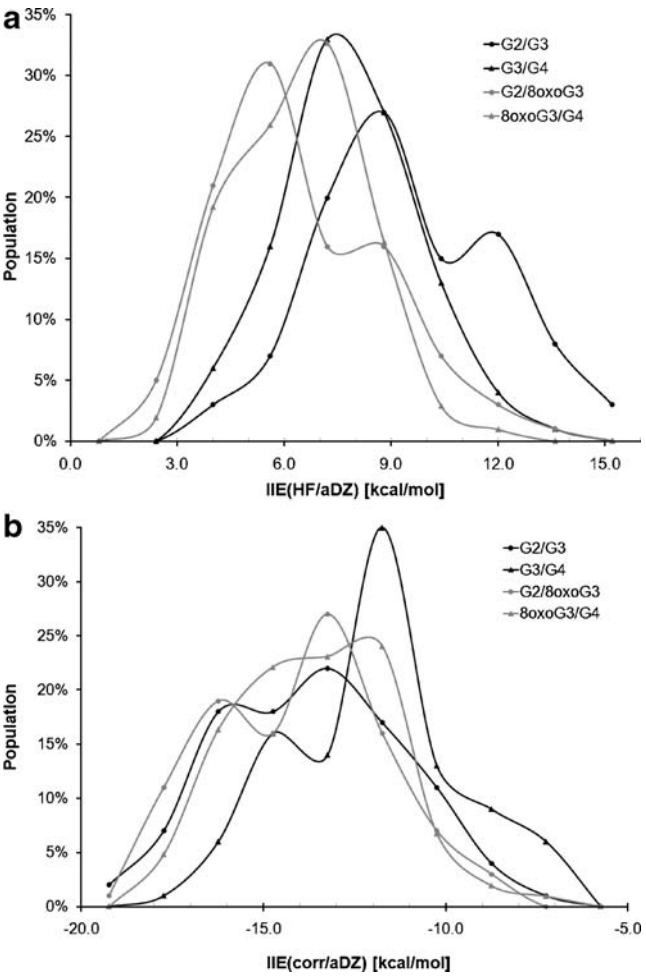

Fig. 5 The distributions of the SCF and electron correlation contributions to the intermolecular interactions energies of stacked pairs in central telomeric fragment

increase of electron correlation in the same magnitude as it is in the case of G_2/G_3.

The relationships between structure and IIE are presented in Fig. 6. The contour maps represent the percentage of structures characterized by values of particular base step parameter and corresponding value of IIE. The method used for preparation of these plots was very similar to one applied to smoothed histograms. Namely, the whole span of values presented on either axis was divided on ten equal intervals and the relative populations were estimated. The scale of colour spectrum is the same for all contour plots in Fig. 6. The six parameters for which the plots were presented are ones that actually define the stacked conformations of two monomers. Additionally, at the edges of the contour maps, the smoothed histograms were supplied for detailed characteristics of distribution of the base step parameters. The grey lines and corresponding grey points typify canonical CTT, while black curves along with black points stand for oxidized CTT. Interestingly, on all presented contour maps almost perfect separation of points is observed representing standard and modified guanine. The source of this feature is the significant differences in the stacking energies. On some of the contour maps there are observed distinct peaks representing the most frequently occurring structures. For example as is demonstrated in Fig. 6a, the interval between 0.3 Å and 1.1 Å of *shift* values is most often used by pairs in oxidized central telomeric fragment. The corresponding peak for canonical CTT is much less pronounced, which again stands for much higher flexibility of non-oxidized B-DNA fragment. Similar conclusion may be also addressed to *roll* and *twist* (Fig. 6e,f). In general the values of all six base step parameters characterizing stacking in canonical telomeric triad fluctuate more significantly than for oxidized CTT. However in cases of *rise* (Fig. 6c)and *tilt* (Fig. 6d) such differences are negligible.

Conclusions

The central guanine triad of telomeric B-DNA repeat unit plays an important role in the interactions with TRF1 and TRF2 ligands. The structural and energetic properties of GGG sequence are significantly affected by oxidation of

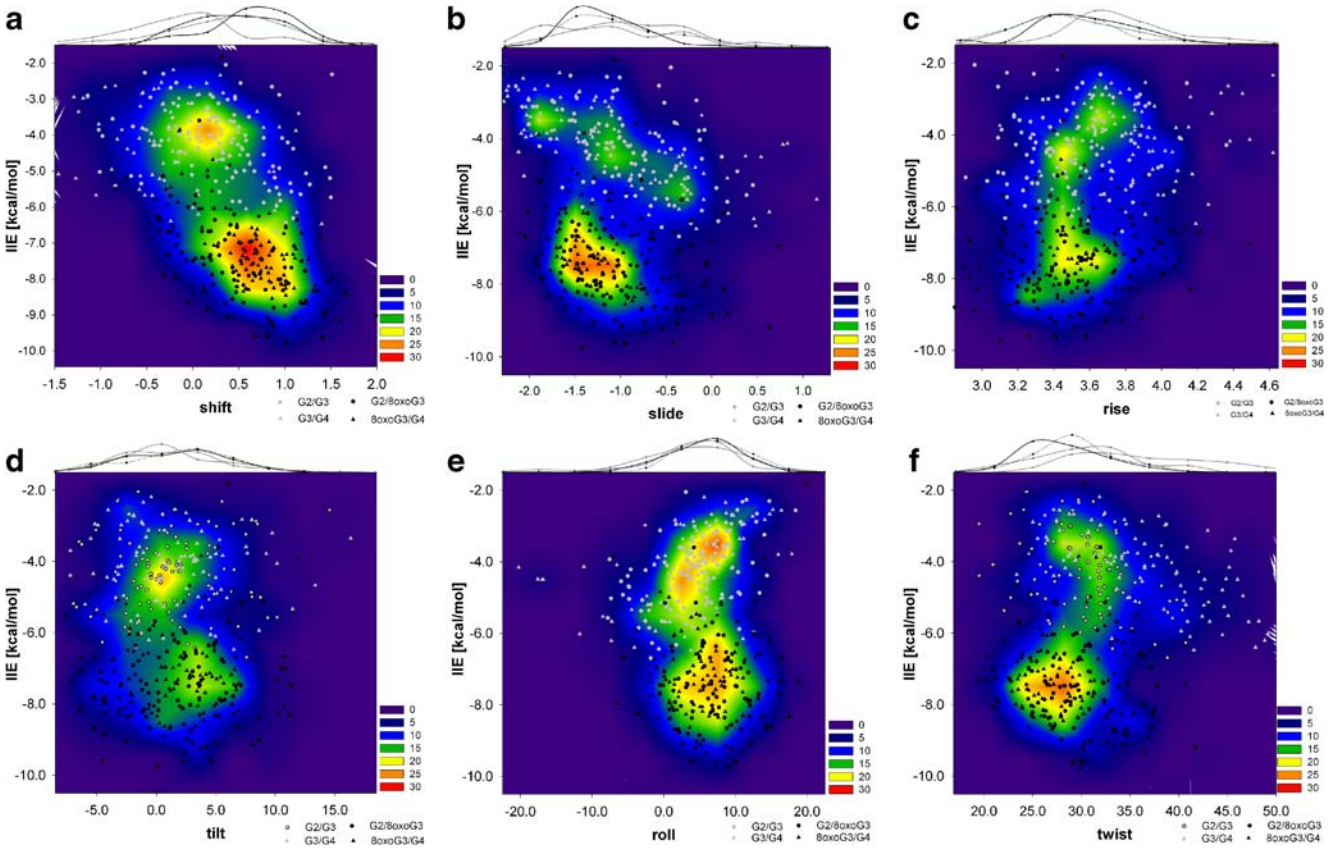

Fig. 6 The contour plots representing correlation between values of base step parameters and IIE of standard and oxidized central telomeric fragments. The colour spectrum represents the percentage of populations characterized by particular value of IIE and *shift*, *slide*, *rise*, *tilt*, *roll* or *twist*. First three displacement parameters are expressed in Angstroms and the last three angular ones are given in degrees

the middle guanine. The results presented above allowed for detailed characteristics of both structure and energy alterations imposed by replacement of middle guanine by its oxidized form at C_8 position. Our analysis has a unique feature, not utilized till now by other investigators. We have combined precise energy estimations on *ab inito* quantum chemistry level with quenching molecular dynamics simulations. This allowed for full statistical analysis of both conformations variability and intermolecular interactions energies heterogeneities. Since the conformations of analyzed pairs exactly mach ones found in B-DNA, the nature of CCT may be directly inferred from our computations. To our best knowledge this kind of information is discussed for the first time. The most important conclusion consistently predicted by structural parameters analysis and IIE distributions is that significant stiffness of central telomeric fragment occurs if 8oxoG is present. This is mainly related to the increase of stacking interactions of 8oxoG with neighbouring guanine molecules. Besides, the significant increase of hydrogen bonding of 8oxoG with cytosine is observed. Both these facts cause a number of structural changes in G8oxoGG fragment if compared to canonical one. Among the most important alterations are reductions of *opening* and *rolling* of pairs comprising the oxidized guanine. Also the distributions of *buckle* indicates increase of stiffness of oxidized central telomeric triad. Another interesting observation is the context independence of stacking interactions of 8oxoG. Unlike to 5′-G_2/G_3-3′ and 5′-G_3/G_4-3′ sequences, which are energetically different, 5′-G/8oxoG-3′ and 5′-8oxoG/G-3′ sequences are almost isoenergetic.

Acknowledgements The results were obtained based on computational grants from PCSS (Poznań Supercomputing and Networking Centre, Poland). The allocation of computing time is greatly appreciated.

References

1. Mathews DH, Sabina J, Zuker M, Turner DHJ (1999) Mol Biol 288:911–940
2. Műller-Dethlefs K, Hobza P (2002) Chem Rev 100:143–167
3. Fairall L, Chapman L, Moss H, de Lange T, Rhodes D (2001) Mol Cell 8:351–361
4. Lundblad V (2000) Mutat Res 451:227–240
5. Harley CB, Futcher AB, Greider CW (1990) Nature 345:458–460
6. von Zglinicki T, Serra V, Lorenz M, Saretzki G, Lenzen-Grossimlighaus R, Gressner R, Risch Steinhagen-Thiessen E (2000) Lab Invest 80:1739–1747
7. Bodnar AG, Ouellette M, Frolkis M, Holt SE, Chiu CP, Morin GB, Harley CB, Shay JW, Lichtsteiner S, Wright WE (1998) Science 279:349–352
8. Chong L, van Steensel B, Broccoli D, Erdjument-Bromage H, Hanish J, Tempst P, de Lange T (1995) Science 270:1663–1667
9. Broccoli D, Smogorzewska A, Chong L, de Lange T (1997) Nat Genet 17:231–235
10. Tchirkov A, Lansdorp PM (2003) Hum Mol Genet 12:227–232
11. von Zglinicki T (2002) Trends Biochem Sci 27:339–344
12. Opresko PL, Fan J, Danzy1 S, David M, Wilson (2005) Nucleic Acids Res 33:1230–1239
13. Cysewski P, Czeleń P (2007) J Mol Model 13:739–750
14. Kabeláč, Sherer EC, Cramer Ch J, Hobza P (2007) Chem Eur J 13:2067–2077
15. Shishkin OV, Šponer J, Hobza P (1999) J Mol Str 477:15–21
16. Gorin AA, Zhurkin VB, Olson WK (1995) J Mol Biol 247:34–48
17. Calladine CR, Drew HR (1986) J Mol Biol 192:907–918
18. Hunter CA (1993) J Mol Bio 230:1025–1054
19. Hill G, Forde G, Hill N, Lester WA Jr, Sokalski WA, Leszczynski (2003) J Chem Phys Lett 381:729–732
20. Hobza P, Šponer J (1999) Chem Rev 99:3247–3276
21. Hobza P, Šponer J, Polaoek M (1995) J Am Chem Soc 117:792–798
22. Sponer J, Hobza P, Leszczyński J (2001) J Mol Str (Teochem) 573:43–53
23. Černý J, Hobza P (2005) Phys Chem Chem Phys 7:1624–1626
24. Hobza P, Sponer J (2002) J Am Chem Soc 124:11802–11808
25. Hanlon S (1966) Biochem Biophys Res Commun 23:861–867
26. Cysewski P, Czyżnikowska Ż, Zaleśny R, Czeleń P (2008) Phys Chem Chem Phys 10:2665–2672
27. Šponer J, Jurečka P, Marchan I, Luque FJ, Orozco M, Hobza P (2006) Chem Eur J 12:2854–2865
28. Kool ET (1997) Chem Rev 97:1473–1487
29. Diekmann S (1989) J Mol Biol 205:787–791
30. Berman HM, Olson WK, Beveridge DL, Westbrook J, Gelbin A, Demeny T, Hsieh SH, Srinivasan AR, Schneider B (1992) Biophys J 63:751–759
31. Fairall L, Chapman L, Moss H, de Lange T, Rhodes D (2001) Mol Cell 8(2):351–61
32. Nishikawa T, Okamura H, Nagadoi A, Konig P, Rhodes D, Nishimura Y (2001) Structure 9:1237–1251
33. Nishikawa T, Nagadoi A, Yoshimura S, Aimoto S, Nishimura Y (1998) Structure 15(6):1057–1065
34. Case DA, Cheatham TE III, Darden T, Gohlke H, Luo R, Merz KM, Onufriev A Jr, Simmerling C, Wang B, Woods R (2005) J Comput Chem 26:1668–1688
35. Lankaš F, Šponer J, Hobza P, Langowski J (2000) J Mol Biol 299:695–709
36. Zacharias M (2006) Biophys J 91(8):882–891
37. Kannan S, Kohlhoff K, Zacharias M (2006) Biophys J 91 (11):2956–2965
38. Mocquet V, Kropachev K, Kolbanovskiy M, Kolbanovskiy A, Tapias A, Cai Y, Broyde S, Geacintov NE, Egly JM (2007) The EMBO J 26:2923–2932
39. Lu XJ, Olson WK (2003) Nucleic Acids Res 31:5108–5121
40. Jansen HB, Ross P (1969) Chem Phys Lett 3:140–143
41. Boys SF, Bernardi F (1970) Mol Phys 19:553–566
42. Case DA, Darden TA, Cheatham TE III, Simmerling CL, Wang J, Duke RE, Luo R, Merz KM, Wang B, Pearlman DA, Crowley M, Brozell S, Tsui V, Gohlke H, Mongan J, Hornak V, Cui G, Beroza P, Schafmeister C, Caldwell JW, Ross WS, Kollman PA (2004) AMBER 8. University of California, San Francisco
43. Werner HJ, Knowles PJ, Lindh R, Manby FR, Schutz M, Celani P, Korona T, Rauhut G, Amos RD, Bernhardsson A, Berning A, Cooper DL, Deegan MJO, Dobbyn AJ, Eckert F, Hampel C, Hetzer G, Lloyd AW, McNicholas SJ, Meyer W, Mura ME, Nicklaß A,Palmieri P, Pitzer R, Schumann U, Stoll H, Stone AJ, Tarroni R, Thorsteinsson T, MOLPRO, a package of ab initio programs designed by Werner HJ and Knowles PJ, Version 2006.0 (Patch 2006.1) Cardiff UK 2006
44. Czyżnikowska Ż, Zaleśny R, Ziółkowski M, Góra RW, Cysewski P (2007) Chem Phys Lett 450:132–137